

# STEMS: Spatial-Temporal Enhanced Safe Multi-Agent Coordination for Building Energy Management

Huiliang Zhang, Di Wu, *Member, IEEE*, Arnaud Zinflou, *Senior Member, IEEE*, and Benoit Boulet, *Senior Member, IEEE*

**Abstract**—Building energy management is essential for achieving carbon reduction goals, improving occupant comfort and reducing energy costs. Coordinated building energy management faces critical challenges in exploiting spatial-temporal dependencies while ensuring operational safety across multi-building systems. Current multi-building energy systems face three key challenges: insufficient spatial-temporal information exploitation, lack of rigorous safety guarantees, and system complexity. This paper proposes Spatial-Temporal Enhanced Safe Multi-Agent Coordination (STEMS), a novel safety-constrained multi-agent reinforcement learning framework for coordinated building energy management. STEMS integrates two core components: (1) a spatial-temporal graph representation learning framework using GCN-Transformer fusion architecture to capture inter-building relationships and temporal patterns, and (2) a safety-constrained multi-agent RL algorithm incorporating Control Barrier Functions to provide mathematical safety guarantees. Extensive experiments on real-world building datasets demonstrate STEMS’s superior performance over existing methods, showing that STEMS achieves 21% cost reduction, 18% emission reduction, and dramatically reduces safety violations from 35.1% to 5.6% while maintaining optimal comfort with only 0.13 discomfort proportion. The framework also demonstrates strong robustness during extreme weather conditions and maintains effectiveness across different building types.

**Index Terms**—Building Energy Management, Multi-agent, Reinforcement Learning, Spatial-Temporal Graph Networks, Safety Constraints.

## I. INTRODUCTION

Buildings consume approximately 40% of global energy and account for 36% of CO<sub>2</sub> emissions worldwide [1]. This massive energy consumption directly impacts environmental sustainability and economic costs as urbanization accelerates. Moreover, as urban residents spend over 80% of their time indoors, building energy management directly affects daily life quality. People require comfortable indoor environments under safe building control while facing rising energy costs and environmental concerns. This creates a complex multi-objective optimization challenge where comfort, safety, economic efficiency, and environmental sustainability must be balanced simultaneously [2]. Current building energy management sys-

Huiliang Zhang, Di Wu, and Benoit Boulet are with the Department of Electrical Computer Engineering, McGill University, Montreal, QC H3A 0G4, Canada (e-mail: huiliang.zhang2@mail.mcgill.ca; di.wu5@mcgill.ca; benoit.boulet@mcgill.ca).

Arnaud Zinflou is with the Data Science Team, Institut de Recherche Hydro Québec, Montreal, QC, Canada (e-mail: zinflou.arnaud@hydroquebec.com).

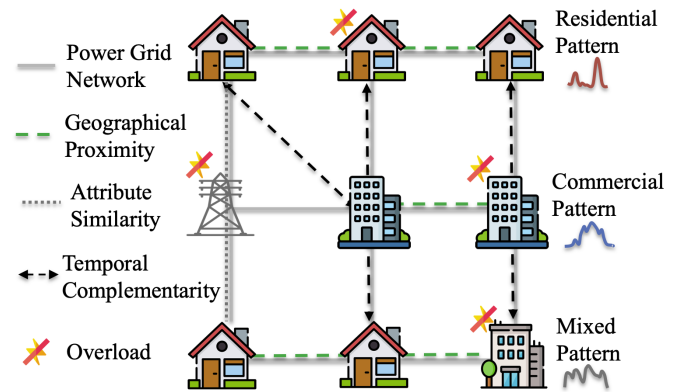


Fig. 1: Complex spatial-temporal relationships and energy consumption patterns in multi-building systems: challenges of uncoordinated control and potential safety violations.

tems operate independently among individual buildings, which limits their ability to achieve optimal performance [3].

The widespread deployment of smart sensors and IoT devices has enabled buildings to monitor real-time conditions and share information about energy demand, storage status, and operational strategies. This information sharing capability opens new ways for coordinated energy management across building clusters. Reinforcement learning (RL) provides a promising solution for building energy management because it can learn optimal control policies without requiring precise system models. Unlike traditional model predictive control (MPC) methods that rely on accurate mathematical models, RL algorithms can adaptively learn through interaction with the environment, handling system uncertainties and complexities effectively. In multi-building scenarios, each building can act as an intelligent agent, enabling coordinated optimization through multi-agent reinforcement learning (multi-agent RL). Multi-agent RL allows buildings to learn collaborative strategies while maintaining individual autonomy, making it particularly suitable for distributed energy management systems. However, applying multi-agent RL to building energy management still faces three critical challenges:

- **Insufficient spatial-temporal information exploitation:** Current approaches fail to effectively exploit spatial-temporal information in building energy systems [4], [5]. As shown in Figure 1, buildings exhibit multiple types of

relationships alongside their distinct energy consumption patterns. The spatial relationships include geographical proximity, attribute similarity, and temporal complementarity among different building types. Buildings close to each other will have heat transfer and shading effects among neighboring structures, residential buildings show double-peak patterns with morning and evening usage spikes, while commercial buildings maintain relatively stable consumption during business hours. However, existing methods ignore those hidden dependencies and patterns that are crucial for coordinated decision-making. Without proper spatial-temporal feature extraction and modeling mechanisms, buildings make decisions based on limited local observations, leading to suboptimal performance. For example, during summer peak hours, all buildings independently decide to pre-cool their spaces before peak pricing begins. This simultaneous cooling demand overloads the electrical grid, causing supply instability and higher costs for everyone.

- **Lack of rigorous safety guarantees:** Existing control methods lack rigorous safety guarantees [6], [7] or rely on soft constraints, such as penalty terms in RL algorithms, to discourage unsafe behaviors. However, these methods cannot provide mathematical guarantees against constraint violations [8]. During the learning and exploration process, control systems may still conduct unsafe actions such as exceeding battery capacity limits or unit power outage. Moreover, when buildings operate as isolated islands with limited local observations and broken information connections, they are more likely to exhibit safety warnings and uncoordinated consumption patterns, leading to power grid-level equipment damage risks and overloads, resulting in significant economic losses.
- **System complexity and algorithmic challenges:** The inherent complexity of building energy systems poses significant algorithmic challenges for coordination [9], [10]. As illustrated in Figure 1, the diverse building types and their complex interaction patterns create a challenging optimization landscape. Multi-objective optimization requirements involving comfort, efficiency, and safety lead to complex trade-offs that are difficult to balance simultaneously [11]. The rapid development of distributed storage and renewable energy systems creates dynamic and uncertain environments with intermittent generation and variable demand patterns. These factors, combined with the instability of RL algorithms in high-dimensional continuous spaces, make convergence slow and solution quality unpredictable [12], [13].

To address these multi-agent RL challenges in building energy management, this paper proposes Spatial-Temporal Enhanced Safe Multi-Agent Coordination (STEMS), a novel spatial-temporal aware safe multi-agent reinforcement learning framework for coordinated building energy management. Our approach consists of two key components that work together to overcome the identified limitations. First, we develop a spatial-temporal graph representation learning framework that effec-

tively captures the complex relationships among buildings. We propose a GCN-Transformer fusion architecture that processes both spatial dependencies through graph convolution and temporal patterns through attention mechanisms. This framework includes a selective information construction mechanism that enables intelligent collaboration among buildings by dynamically determining what information to share based on spatial-temporal contexts. The approach effectively handles high-dimensional state spaces through structured feature extraction and dimensionality reduction. Second, we design a safety-constrained multi-agent RL algorithm that provides mathematical guarantees for safe operation. We integrate Control Barrier Functions (CBFs) [8] as safety shields that ensure control actions remain within safe operating bounds. The algorithm incorporates a predictive safety checking mechanism that prevents unsafe actions from being executed while maintaining system performance. This enables precise safety control in continuous action spaces, addressing the critical need for reliable operation in real-world building energy systems. In summary, the main contributions of this work are threefold:

- We design a novel GCN-Transformer fusion module that effectively processes spatial-temporal dependencies with shared spatial and temporal information among buildings to improve the situation awareness and decision-making in building energy management systems.
- We propose a constrained multi-agent RL framework that integrates CBFs to provide mathematical guarantees for safe operation in building energy management.
- We validate that STEMS significantly improves energy efficiency and economic performance through extensive experiments on real-world building energy datasets. The results demonstrate the effectiveness of our spatial-temporal aware approach and the importance of safety constraints in coordinated building energy management. STEMS achieves substantial improvements over existing approaches in both energy savings and cost reduction.

The remainder of this paper is organized as follows. Section II reviews related work in building energy management, spatial-temporal modeling, and safe multi-agent RL. Section III formulates the problem and presents our system model for coordinated building energy management. Section IV details our proposed spatial-temporal graph representation learning framework and safety-constrained multi-agent RL algorithm. Section V presents comprehensive experimental results and analysis on real-world building energy datasets. Section VI concludes the paper and discusses future research directions.

## II. SYSTEM MODEL AND METHODOLOGY

### A. Problem Formulation

We consider a multi-building energy management system composed of  $N$  buildings, denoted as the building set  $\mathcal{B} = \{B_1, B_2, \dots, B_N\}$ . Each building is equipped with smart sensors and communication devices. This enables real-time monitoring of operational states and information sharing with neighboring buildings. The system includes diverse building types: residential, commercial, and mixed-use facilities. These

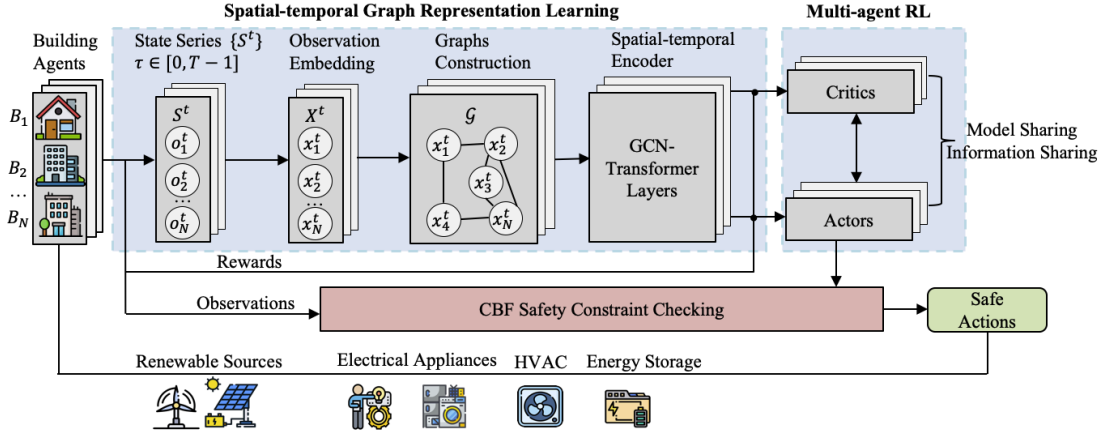


Fig. 2: STEMS Framework. Building agents collect state observations, which are processed through spatial-temporal graph learning to extract inter-building relationships and temporal patterns. The multi-agent RL module generates coordinated control actions, which are verified by CBF safety constraints before execution, with resulting rewards guiding the learning of RL.

buildings are distributed across geographical space with potential physical coupling relationships.

The inter-building relationships are represented by a communication graph  $\mathcal{G} = (\mathcal{N}, \mathcal{E})$ , where  $\mathcal{N}$  denotes the node set (buildings) and  $\mathcal{E}$  represents the edge set (connection relationships). Connection relationships between buildings are determined through two primary approaches: geographical proximity calculation based on Euclidean distance, and attribute similarity calculation based on building characteristics and usage patterns. The neighbor set of building  $B_i$  is denoted as  $\mathcal{N}_i$ , representing buildings that can engage in information exchange.

The multi-building energy management challenge is formulated as a constrained multi-agent RL problem, defined by the tuple:

$$\mathcal{M} = (\mathcal{S}, \mathcal{A}, \mathcal{P}, \mathcal{R}, \mathcal{C}, \mathcal{G}, \gamma) \quad (1)$$

where  $\mathcal{G} = (\mathcal{N}, \mathcal{E})$  represents the inter-building communication network,  $\mathcal{R} = \{R_i\}$  denotes the reward function set,  $\mathcal{C} = \{C_i\}$  represents the constraint function set, and  $\gamma$  is the discount factor.

Each building agent observes a state space  $\mathcal{S}_i = \{o_i, o_{j \in \mathcal{N}_i}\}$  that combines self-observations  $o_i$  (including internal device states, environmental conditions, and economic signals) with shared information  $o_{j \in \mathcal{N}_i}$  from neighboring buildings. The action space  $\mathcal{A}_i$  are continuous control decisions for energy storage systems, Heating, Ventilation, and Air Conditioning (HVAC) operations, and other controllable devices. The system aims to optimize long-term performance through reward functions  $R_i$  that balance economic efficiency and operational stability, while satisfying safety constraints  $C_i$  that ensure reliable and secure operation.

The optimization objective for each building agent is to learn an optimal policy  $\pi_i^* : \mathcal{S}_i \mapsto \mathcal{A}_i$  that maximizes expected cumulative rewards:

$$\pi_i^* = \arg \max_{\pi_i} \mathbb{E} \left[ \sum_{t=0}^T \gamma^t R_t^i \mid \pi_i \right] \quad (2)$$

subject to safety constraints:  $\mathbb{E}[C_i(s_t, a_t)] \geq 0, \forall t$ . The safety constraints  $C_i(s_t, a_t)$  include battery safety limits, power capacity constraints, and grid stability conditions, which are detailed in Section II-D.

### B. Overall Framework

To simultaneously address spatial-temporal dependency modeling, safety constraint guarantees, and multi-objective optimization challenges in building energy management, STEMS adopts a modular design that integrates three synergistic core components: the spatial-temporal graph representation learning module, the CBF safety constraint checking module, and the multi-agent RL module. Figure 2 illustrates the overall architecture and information flow among these components. Initially, building agents collect comprehensive state observations  $\mathcal{S}$  including internal device status, environmental conditions, and neighboring building information. These observations are then processed by the spatial-temporal graph representation learning module through observation embeddings, graph convolution and temporal attention layers to extract spatial-temporal features that capture inter-building relationships and temporal patterns. Subsequently multi-agent RL utilizes these enhanced spatial-temporal features to generate control actions  $\mathcal{A}$  for each building through coordinated decision-making, where the rewards  $\mathcal{R}$  and state transitions guide the continuous learning process.

The CBF safety constraint checking module verifies that all proposed actions satisfy operational safety requirements. Once safe actions are executed in the environment, the resulting performance is evaluated through a multi-objective reward function that balances four key objectives:

$$R_t^i = R_{economic}^i + R_{stability}^i + R_{comfort}^i + R_{renewable}^i \quad (3)$$

For building  $i$  at time step  $t$ , the net electricity consumption is:

$$e_t^i = b_t^i + P_{HVAC,t}^i + P_{batt,t}^i - p_t^i \quad (4)$$

where  $b_t^i$  represents non-shiftable loads,  $P_{HVAC,t}^i$  denotes HVAC power demand,  $P_{batt,t}^i$  indicates battery charging/discharging power, and  $p_t^i$  represents renewable energy generation.

The economic efficiency component minimizes electricity costs:

$$R_{economic}^i = -\mu \cdot v_t \cdot e_t^i \quad (5)$$

The stability component combines grid-level coordination and building-level smooth operation:

$$R_{stability}^i = \alpha_{grid} \cdot \left( 1 - \frac{\sum_{j=1}^N \max(0, e_t^j)}{P_{grid,max}} \right)^2 + \alpha_{build} \cdot \left( 1 - \frac{|e_t^i|}{P_{building,max}^i} \right) \quad (6)$$

$$- \beta_{ramp} \cdot \frac{|e_t^i - e_{t-1}^i|}{P_{building,max}^i} \quad (7)$$

The comfort component maintains indoor temperature close to user preferences:

$$R_{comfort}^i = -\lambda_{indoor} \cdot |T_t^{in,i} - T_{ref}^i|^2 \quad (8)$$

The renewable energy component maximizes clean energy utilization:

$$R_{renewable}^i = \xi \cdot \min \left( \frac{p_t^i}{p_t^i + \max(0, e_t^i)}, 1 \right) \quad (9)$$

These four components work together to achieve balanced performance. The economic term minimizes electricity costs by optimizing consumption timing and renewable energy use. For system stability, the grid-level coordination with smooth building operations helps buildings work together to avoid overloads while maintaining steady power consumption. The comfort term allows flexible trade-offs between energy efficiency and occupant comfort based on real-time conditions and the renewable component maximizes clean energy utilization across all buildings.

### C. Spatial-Temporal Graph Representation Learning Framework

The spatial-temporal graph representation learning framework captures the complex interdependencies among buildings and their temporal evolution patterns to enhance decision-making capabilities. This framework leverages graph neural networks to encode spatial relationships and temporal attention mechanisms to model dynamic patterns in energy consumption and environmental conditions.

1) *Graph Construction and Node Features*: The building interaction graph  $\mathcal{G}_{build} = (\mathcal{V}, \mathcal{E}_{build})$  is constructed where each node represents a building and edges encode interaction relationships. Node features for building  $i$  at time  $t$  include:

$$\mathbf{x}_i^t = [\mathbf{s}_i^t, \mathbf{e}_i^t, \mathbf{c}_i^t] \quad (10)$$

where  $\mathbf{s}_i^t$  represents building state features (State of Charge (SOC), indoor temperature, device status),  $\mathbf{e}_i^t$  denotes environmental features (outdoor temperature, solar irradiance,

electricity price), and  $\mathbf{c}_i^t$  captures building characteristics (type, capacity, efficiency parameters).

Edge weights are computed based on the connection strength between buildings:

$$w_{ij} = \alpha \cdot \exp \left( -\frac{d_{ij}^2}{2\sigma_d^2} \right) + \beta \cdot \exp \left( -\frac{\|\mathbf{f}_i - \mathbf{f}_j\|^2}{2\sigma_f^2} \right) \quad (11)$$

where  $d_{ij}$  represents geographical distance,  $\mathbf{f}_i$  and  $\mathbf{f}_j$  are building attribute vectors, and  $\alpha, \beta$  are weighting parameters for geographical and attribute-based similarities.

2) *Spatial Feature Encoding*: Graph convolutional layers aggregate information from neighboring buildings to capture spatial dependencies in energy consumption patterns. The spatial encoding for building  $i$  at layer  $l$  is computed as:

$$\mathbf{h}_i^{(l+1)} = \sigma \left( \mathbf{W}^{(l)} \sum_{j \in \mathcal{N}_i \cup \{i\}} \frac{w_{ij}}{\sqrt{d_i d_j}} \mathbf{h}_j^{(l)} \right) \quad (12)$$

where  $\mathbf{h}_i^{(l)}$  represents the hidden state of building  $i$  at layer  $l$ ,  $\mathbf{W}^{(l)}$  is the learnable weight matrix,  $d_i$  is the degree of node  $i$ , and  $\sigma$  is the activation function.

3) *Temporal Pattern Modeling*: A multi-head attention mechanism captures temporal dependencies in building energy consumption and environmental patterns. For building  $i$ , the temporal attention weights are computed as:

$$\alpha_{i,t,\tau} = \frac{\exp(\mathbf{q}_{i,t}^T \mathbf{k}_{i,\tau})}{\sum_{\tau'=t-T}^t \exp(\mathbf{q}_{i,t}^T \mathbf{k}_{i,\tau'})} \quad (13)$$

where  $\mathbf{q}_{i,t}$  and  $\mathbf{k}_{i,\tau}$  are query and key vectors derived from building states, and  $T$  is the temporal window size.

The temporal representation is obtained through weighted aggregation:

$$\mathbf{z}_i^t = \sum_{\tau=t-T}^t \alpha_{i,t,\tau} \mathbf{v}_{i,\tau} \quad (14)$$

where  $\mathbf{v}_{i,\tau}$  represents the value vector at time  $\tau$ .

The final spatial-temporal representation combines spatial and temporal features:

$$\mathbf{r}_i^t = \mathbf{W}_s \mathbf{h}_i^{(L)} + \mathbf{W}_t \mathbf{z}_i^t + \mathbf{b} \quad (15)$$

where  $\mathbf{W}_s$  and  $\mathbf{W}_t$  are learnable projection matrices, and  $\mathbf{b}$  is the bias term.

### D. Safety-Constrained Decision Making

Building energy systems require strict safety constraints to prevent equipment damage and ensure reliable operation. Battery overcharging can cause thermal runaway and fire hazards. Power overloads can damage electrical equipment and cause grid instability.

Our safety-constrained approach ensures these critical requirements are never violated during both training and deployment. Unlike penalty-based methods that may still produce unsafe actions during exploration, we use CBFs to mathematically guarantee constraint satisfaction.

**1) Control Barrier Function Framework:** To enforce the safety constraints  $c_i(s_t, a_t) \geq 0$  defined in the problem formulation, we construct corresponding CBFs that provide implementable constraint enforcement mechanisms. We define three key safety constraints for building energy management:

**Battery Safety:** Energy storage must operate within safe SOC limits to prevent thermal runaway and equipment damage:

$$h_{battery}^i(s, a) = \min(SOC_{max} - SOC_{t+1}^i, SOC_{t+1}^i - SOC_{min}) \geq 0 \quad (16)$$

**Building Safety:** Building power consumption cannot exceed capacity to prevent equipment overload and local outages:

$$h_{power}^i(s, a) = P_{building,max}^i - |e_t^i| \geq 0 \quad (17)$$

**Grid Safety:** Total system load must stay within grid limits to maintain system stability:

$$h_{grid}(s, a) = P_{grid,max} - \sum_{i=1}^N \max(0, e_t^i) \geq 0 \quad (18)$$

The battery state will be updated with:  $SOC_{t+1}^i = SOC_t^i + \frac{a_t^i \cdot \Delta t}{Capacity_i}$ .

For each continuous action  $a_t^i \in \mathbb{R}^{|\mathcal{A}_i|}$  generated by the actor network, we conduct safety verification, which is detailed in Algorithm 1, ensuring that all building control actions satisfy safety constraints before execution.

First, we evaluate whether the proposed action directly satisfies all safety constraints:

$$h_j(s_t, a_t^i) \geq 0, \quad \forall j \in \{\text{battery, power, grid}\} \quad (19)$$

If all constraints are satisfied, the action is executed directly:  $a_t^{i,safe} = a_t^i$ .

Then, if any constraint is violated, we solve the CBF-quadratic programming (QP) optimization problem to find the closest safe action:

$$a_t^{i,safe} = \arg \min_u \frac{1}{2} \|u - a_t^i\|^2 \quad \text{s.t. } h_j(s_t, u) \geq 0, \forall j \quad (20)$$

This ensures the executed action is as close as possible to the original policy output while maintaining safety. If it is feasible, the action is safe. Otherwise, emergency conservative actions will be applied.

The safe action space is defined as:

$$\mathcal{A}_i^{safe} = \{a \in \mathcal{A}_i : \text{safety constraints satisfied}\} \quad (21)$$

This approach provides mathematical guarantees that safety constraints are never violated, ensuring reliable building energy management operations.

#### E. Multi-Agent Training Algorithm

The proposed safety-constrained multi-agent RL algorithm integrates the spatial-temporal graph representation learning framework with safety constraint enforcement to achieve coordinated and safe energy management across multiple buildings. The complete training procedure is detailed in

Algorithm 2, which shows the interaction between spatial-temporal learning, safety verification, and policy optimization.

**Actor-Critic Architecture:** Each building agent  $i$  employs an actor-critic architecture where the actor network  $\pi_\theta^i$  generates control actions and the critic network  $V_\phi^i$  estimates state values. The spatial-temporal representation  $\mathbf{r}_i^t$  serves as input to both networks:

$$a_t^i = \pi_\theta^i(\mathbf{r}_i^t) + \epsilon_t \quad (22)$$

$$V_t^i = V_\phi^i(\mathbf{r}_i^t) \quad (23)$$

where  $\epsilon_t$  represents exploration noise and  $\theta, \phi$  are network parameters.

---

#### Algorithm 1 Multi-Building Safety Verification

---

**Input:** Continuous actions  $\{a_t^i\}_{i=1}^N$  from actor networks, current state  $s_t$

**Output:** Safe actions  $\{a_t^{i,safe}\}_{i=1}^N$

```

1: for each building  $i = 1$  to  $N$  do
2:   Check if  $h_j(s_t, a_t^i) \geq 0, \forall j \in \{\text{battery, power, grid}\}$ 
3:   if All constraints satisfied then
4:      $a_t^{i,safe} = a_t^i$ 
5:   else
6:     Solve CBF-QP:  $\min_u \frac{1}{2} \|u - a_t^i\|^2$  s.t.  $h_j(s_t, u) \geq 0, \forall j$ 
7:     if CBF-QP has feasible solution then
8:        $a_t^{i,safe} = \text{optimal solution}$ 
9:     else
10:      Apply emergency actions based on constraint
11:      violation type
12:       $a_t^{i,safe} = \text{emergency action}$ 
13:    end if
14:  end for
15: return  $\{a_t^{i,safe}\}_{i=1}^N$ 
```

---

**Policy Update:** The actor network is updated using the policy gradient with safety-constrained rewards:

$$\nabla_\theta J(\theta) = \mathbb{E}_{s, a \sim \mathcal{A}^{safe}} [\nabla_\theta \log \pi_\theta(a|s) \cdot A(s, a)] \quad (24)$$

where  $A(s, a) = R(s, a) + \gamma V_\phi(s') - V_\phi(s)$  is the advantage function, and the expectation is taken only over the safe action space.

**Critic Update:** The critic network is updated to minimize the temporal difference error:

$$L(\phi) = \mathbb{E}_{s, a \sim \mathcal{A}^{safe}} [(R(s, a) + \gamma V_\phi(s') - V_\phi(s))^2] \quad (25)$$

**Graph Representation Update:** The spatial-temporal graph representation parameters are updated end-to-end through backpropagation from the actor-critic losses:

$$\nabla_\psi L_{total} = \nabla_\psi J(\theta) + \nabla_\psi L(\phi) \quad (26)$$

where  $\psi$  represents the parameters of the graph neural network components.

This integrated approach ensures that the learned policies not only optimize performance but also maintain strict adherence to safety requirements throughout the learning process.

**Algorithm 2** Safety-Constrained Multi-Agent Training

---

**Input:** Initial policy parameters  $\{\theta^i\}_{i=1}^N$ , critic parameters  $\{\phi^i\}_{i=1}^N$ , graph parameters  $\psi$   
**Output:** Trained policy networks  $\{\pi_{\theta^i}^*\}_{i=1}^N$

- 1: **for** episode  $e = 1$  to  $E_{max}$  **do**
- 2:   Initialize environment and building states  $\{s_0^i\}_{i=1}^N$
- 3:   **for** time step  $t = 0$  to  $T - 1$  **do**
- 4:     Compute spatial-temporal representations  $\{\mathbf{r}_t^i\}_{i=1}^N$  using graph networks
- 5:     Generate raw actions  $\{a_t^i\}_{i=1}^N$  from actor networks  $\{\pi_{\theta^i}\}_{i=1}^N$
- 6:     Apply Algorithm 1 to get safe actions  $\{a_t^{i,safe}\}_{i=1}^N$
- 7:     Execute safe actions and observe rewards  $\{R_t^i\}_{i=1}^N$  and next states  $\{s_{t+1}^i\}_{i=1}^N$
- 8:     Store experience tuples  $\{(s_t^i, a_t^{i,safe}, R_t^i, s_{t+1}^i)\}_{i=1}^N$
- 9:   **end for**
- 10:   Compute advantage functions  $\{A_t^i\}$  using critic networks
- 11:   Update actor networks using policy gradient:  $\theta^i \leftarrow \theta^i + \alpha_\pi \nabla_{\theta^i} J(\theta^i)$
- 12:   Update critic networks using TD error:  $\phi^i \leftarrow \phi^i + \alpha_v \nabla_{\phi^i} L(\phi^i)$
- 13:   Update graph parameters end-to-end:  $\psi \leftarrow \psi + \alpha_g \nabla_\psi L_{total}$
- 14:   **if** episode  $e \bmod K = 0$  **then**
- 15:     Adjust safety constraint parameters based on system performance
- 16:   **end if**
- 17: **end for**
- 18: **return** Trained policy networks  $\{\pi_{\theta^i}^*\}_{i=1}^N$

---

The spatial-temporal graph representation enables effective coordination among buildings, while the safety constraint enforcement provides reliable operation guarantees.

### III. EXPERIMENTS

In this section, we evaluate our proposed STEMS method for coordinated building energy management. We first present the experimental settings including simulation environment, baseline methods, and evaluation metrics. Then we analyze the experimental results to demonstrate the effectiveness of our approach.

#### A. Experimental Setup

1) *Simulation Environment*: We conduct experiments based on the CityLearn environment[14], a multi-building energy management simulation platform that provides realistic building energy dynamics and grid interactions. The experimental dataset is derived from real building energy consumption data in Travis County, Texas. The dataset spans from August 2018 to August 2019, capturing a full year of operation under typical subtropical humid climate conditions: annual average temperature of  $20.7^{\circ}\text{C}$ , temperature range from  $-7.8^{\circ}\text{C}$  to  $42.8^{\circ}\text{C}$ . This climate profile creates significant cooling-dominated energy demands during summer months and moderate heating requirements in winter, providing realistic conditions for

evaluating multi-building energy coordination strategies. The data includes 1 hour interval measurements of electricity consumption, solar generation, battery storage, and environmental conditions. The experimental setup consists of 8 buildings in a neighborhood configuration with typical regional distribution (5 residential, 2 commercial, 1 mixed-use). The 8 buildings are randomly selected from the Travis County dataset based on above ratio to ensure representative diversity in building characteristics and energy consumption patterns. Most residential buildings show dual-peak patterns with morning (6-9h) and evening (18-22h) usage spikes, reflecting typical household activities with strong seasonal variations. Commercial buildings demonstrate business-hour concentrated loads (9-17h) with midday peaks around 12-13h. Mixed-use buildings combine both residential and commercial characteristics with variable all-day consumption patterns. Each building is equipped with controllable devices including battery energy storage systems (BESS), HVAC systems, solar photovoltaic panels, hot water tank. Buildings can communicate with each other to share state information and coordinate energy management decisions.

2) *Baseline Methods*: We compare our method (STEMS) against the following baseline methods:

**Rule-Based**: Traditional rule-based control using time-of-use scheduling and temperature setpoint control.

**MPC**: Model Predictive Control using linear building thermal models and quadratic cost functions.

**Single-Agent SAC**: Independent Soft Actor-Critic reinforcement learning for each building without coordination[15].

**MADDPG**: Multi-Agent Deep Deterministic Policy Gradient with centralized training and decentralized execution[16].

**MetaEMS**: Meta-learning based energy management system using Model-Agnostic Meta-Learning (MAML) framework[17].

**MARLISA**: Multi-Agent Reinforcement Learning with Independent Soft Actor-Critic operating independently[12].

3) *Evaluation Metrics*: We evaluate methods using the following key performance metrics:

**Cost**: Total electricity cost including energy charges and demand charges.

**Emission**: Carbon emissions from electricity consumption based on grid carbon intensity.

**Avg. Daily Peak**: Average of maximum daily power demand across all buildings:

$$P_{avg} = \frac{1}{D} \sum_{d=1}^D \max_{t \in d} \sum_{i=1}^N e_{i,t}$$

where  $D$  is the number of days and  $N$  is the number of buildings.

**Electricity Consumption**: Total electricity consumption from the grid.

**Ramping Rate**: Grid load change rate measuring power fluctuations:

$$R = \frac{1}{T-1} \sum_{t=2}^T |e_t - e_{t-1}|$$

where  $e_t$  is the total grid load at time  $t$ .

**Discomfort Proportion:** Percentage of time when indoor temperature is outside the comfort range [20°C, 26°C]:

$$D_{prop} = \frac{1}{T \cdot N} \sum_{t=1}^T \sum_{i=1}^N \mathbf{1}(T_{i,t} < 20 \text{ or } T_{i,t} > 26)$$

where  $T_{i,t}$  is the indoor temperature of building  $i$  at time  $t$ .

**Safety Violations(%):** Percentage of safety constraint violations including battery SOC limits, thermal comfort bounds, and equipment operation constraints.

All metrics except Safety Violations are normalized relative to the rule-based baseline performance to enable fair comparison across different methods and scenarios.

*4) Implementation Details:* All algorithms are implemented in Python using PyTorch. The training dataset contains 8760 time steps covering a full year of operation with 1-hour intervals. The graph neural network uses 3 layers with 64 hidden units each. The temporal attention mechanism has 4 heads with 32-dimensional embeddings. Actor and critic networks have 2 hidden layers with 128 units each. The weighting parameters are:  $\mu = 1.0$  (economic baseline),  $\alpha_{grid} = 0.5$  (grid stability),  $\alpha_{build} = 0.3$  (building stability),  $\beta_{ramp} = 0.2$  (power ramp penalty),  $\lambda_{indoor} = 0.4$  (indoor comfort), and  $\xi = 0.6$  (renewable energy). Training uses the Adam optimizer with learning rate  $3 \times 10^{-4}$ . The discount factor  $\gamma$  is set to 0.99. The model converges within 15 epochs, with each epoch taking approximately 3 minutes. Total training time is approximately 45 minutes on an NVIDIA RTX 5090 GPU. All baseline methods are implemented following their original paper parameters and fine-tuned to achieve optimal performance in our experimental setting.

### B. Performance Evaluation

We evaluate the learned policies after training completion. All reported metrics are computed using the converged policies during evaluation episodes, averaged over 5 random seeds to ensure statistical reliability. Table I presents the long-term performance comparison based on 12 months of continuous operation data. The results represent averaged performance across different seasons and weather conditions, demonstrating the sustained effectiveness of STEMS in real-world deployment.

Over the 12-month evaluation period, STEMS demonstrates sustained superior performance across almost all metrics compared to baseline methods. Traditional control approaches exhibit significant limitations in economic aspects in multi-building coordination. Rule-based control also suffers from rigid scheduling policies that cannot adapt to dynamic conditions, resulting in the highest safety violation rate (35.1%). MPC, while offering some optimization capability, is limited by its reliance on simplified linear models and lacks coordination mechanisms, achieving only modest improvements with 33.0% safety violations and high discomfort proportion. For learning-based baselines, Single-Agent SAC, despite showing competitive economic performance (0.82 cost, 0.86 emission), suffers from lack of coordination and safety guarantees, resulting in 22.3% safety violations and

suboptimal comfort management (0.48 discomfort proportion). MADDPG and MetaEMS, while incorporating multi-agent learning, lack explicit safety mechanisms and spatial-temporal modeling, leading to higher safety violation rates (19.7% and 23.1% respectively) and limited comfort optimization. MARLISA achieves reasonable performance but still exhibits 21.4% safety violations due to absence of safety constraints. STEMS's integrated approach combining spatial-temporal graph representation with CBF-based safety mechanisms delivers superior overall performance, while maintaining the lowest safety violation rate (5.6%) and best comfort management (0.13 discomfort proportion).

Then we evaluate the robustness and adaptability of STEMS under challenging conditions over the short-term control, we conduct detailed case studies during specific 2-3 day extreme weather. We select Extreme Weather Scenarios where **Heat Wave**: Outdoor temperature over 35-40°C (occurring 21.6% of the year), cooling demand increased by 150%, solar generation enhanced by 20%. **Cold Wave**: Outdoor temperature under -3°C (occurring 3.0% of the year), heating demand increased by 180%, battery capacity reduced by 15%.

Figure 3 presents a comprehensive performance analysis through radar chart visualization, revealing STEMS's consistent superiority across both extreme weather scenarios. The radar charts display improvement rates relative to Rule-Based baseline, providing intuitive comparison of multi-dimensional performance metrics. In Heat Wave conditions, STEMS achieves remarkable technical improvements: 19% cost reduction, 16% emission reduction, 16% peak demand reduction, 18% consumption reduction, and 10% ramping reduction. The Cold Wave scenario demonstrates similar excellence with 18% cost reduction, 14% emission reduction, 16% peak reduction, 16% consumption reduction, and 11% ramping reduction. The consistent radar chart patterns across both scenarios highlight STEMS's robust adaptability, with the spatial-temporal coordination mechanism effectively handling the contrasting challenges of cooling-dominated Heat Wave periods and heating-intensive Cold Wave conditions.

**Heat Wave Case Study:** During extreme heat conditions (over 35°C outdoor temperature), cooling demand increases by 150% while solar generation is enhanced by 20%, creating significant challenges for energy management systems. The radar chart analysis in Figure 3 demonstrates STEMS's exceptional technical performance, achieving balanced improvements across all metrics. The spatial-temporal coordination enables intelligent scheduling of cooling systems across buildings, avoiding simultaneous activation that would overload the grid. The enhanced solar generation is effectively coordinated across buildings through the spatial graph network, enabling optimal energy sharing and storage scheduling during peak cooling periods. Most notably, as shown in Figure 4, thermal comfort is dramatically improved with STEMS achieving 0.15 discomfort level compared to 0.19 for Rule-Based control (21% improvement), while Figure 5 reveals safety violations are reduced by 77% (from 42.4% to 9.6%).

**Cold Wave Case Study:** Under severe cold conditions (below -3°C), heating demand surges by 180% while battery capacity decreases by 15% due to low-temperature effects. The

TABLE I: Long-term Performance Comparison (12-Month Average Results)

Method	Cost	Emission	Avg. Daily Peak	Electricity Consumption	Ramping Rate	Discomfort Proportion	Safety Violations(%)
Rule-Based	1.00	1.00	1.00	1.00	1.00	0.13	35.1
MPC	0.87	0.91	0.98	0.97	0.98	0.65	33.0
Single-Agent SAC	0.82	0.86	0.85	0.81	0.92	0.48	22.3
MADDPG	0.79	0.81	0.85	0.85	0.93	0.35	19.7
MetaEMS	0.83	0.80	0.88	0.83	0.90	0.39	23.1
MARLISA	0.84	0.87	0.82	0.83	0.95	0.23	21.4
<b>STEMS</b>	<b>0.79</b>	<b>0.82</b>	<b>0.82</b>	<b>0.80</b>	<b>0.88</b>	<b>0.13</b>	<b>5.6</b>

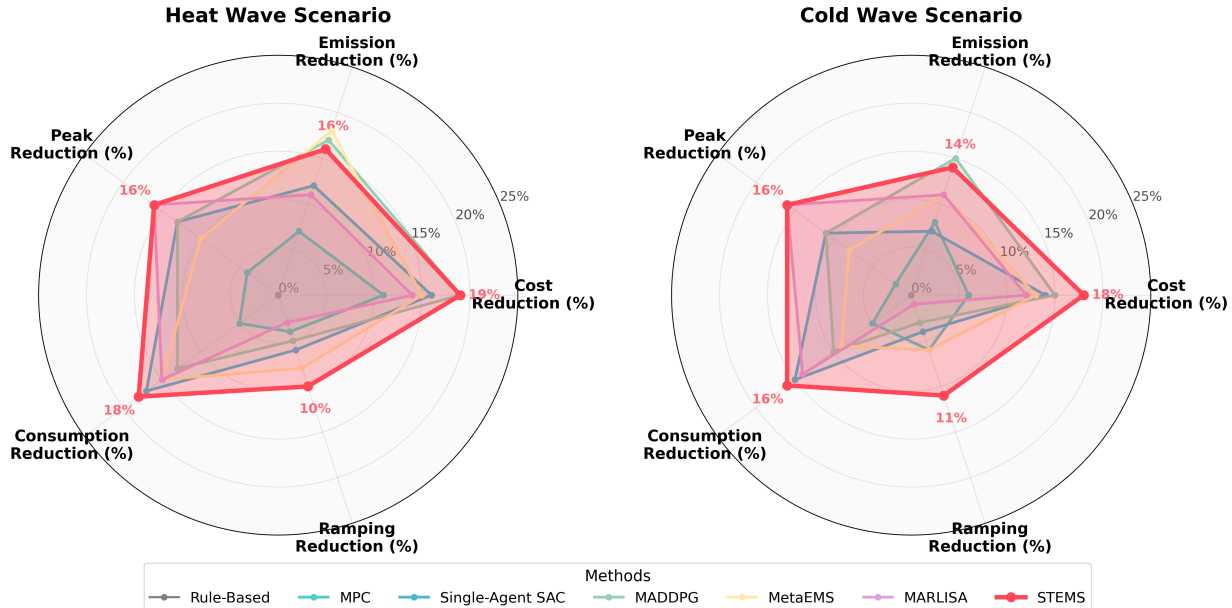


Fig. 3: Performance comparison between Heat Wave and Cold Wave scenarios. The charts display improvement rates relative to Rule-Based baseline across five key technical metrics: Cost Reduction, Emission Reduction, Peak Reduction, Consumption Reduction, and Ramping Reduction. STEMS (highlighted in red) demonstrates consistent superior performance in both extreme weather conditions, achieving 19% cost reduction and 16% peak reduction in Heat Wave scenarios, and 18% cost reduction with 16% peak reduction in Cold Wave scenarios.

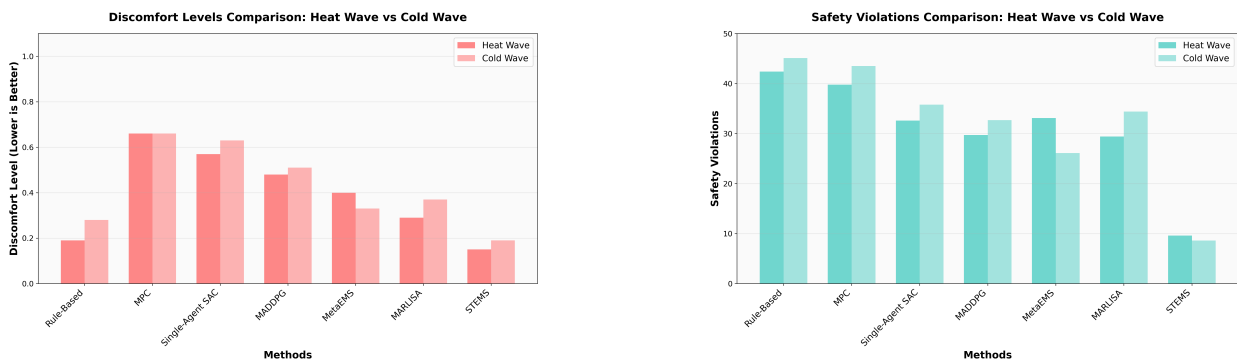


Fig. 4: Discomfort levels comparison between Heat Wave and Cold Wave scenarios across all evaluated methods. STEMS achieves the lowest discomfort levels in both scenarios (0.15 for Heat Wave, 0.19 for Cold Wave), representing 21% and 32% improvement over Rule-Based control respectively. The consistent low discomfort levels demonstrate STEMS's superior thermal comfort management capabilities under extreme weather conditions.

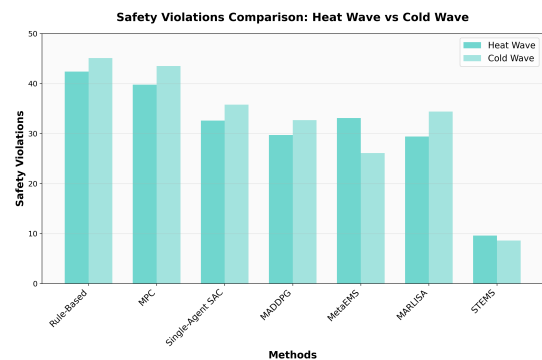


Fig. 5: Safety violations comparison between Heat Wave and Cold Wave scenarios. STEMS maintains the lowest safety violation rates (9.6% for Heat Wave, 8.6% for Cold Wave), representing 77% and 81% reduction compared to Rule-Based control. The CBF-based safety mechanism proves particularly effective in extreme conditions, ensuring operational safety while maintaining performance optimization.

radar chart visualization shows STEMS's adaptive strategy,

maintaining strong performance across all technical metrics despite the challenging operating environment. The algorithm automatically compensates for reduced battery performance by optimizing heating schedules and leveraging inter-building coordination through the learned spatial connections. Figure 4 shows thermal comfort improvement with STEMS achieving 0.19 discomfort level (32% improvement over Rule-Based), while Figure 5 demonstrates safety violations reduced by 81% (from 45.1% to 8.6%). The CBF-based safety mechanism proves particularly valuable in cold conditions, maintaining critical battery and thermal constraints despite the challenging operating environment.

The comprehensive visualization analysis demonstrates STEMS's superior adaptability and robustness across diverse challenging conditions. The radar chart patterns reveal that STEMS maintains high performance levels even when individual components (batteries, HVAC systems) operate under stress, showcasing the value of multi-agent coordination and safety-constrained learning in real-world deployment scenarios. The consistent performance advantage across both extreme weather scenarios, combined with exceptional comfort management and safety assurance, validates STEMS's practical viability for real-world building energy management systems operating under climate variability and extreme weather events.

### C. System Visualization

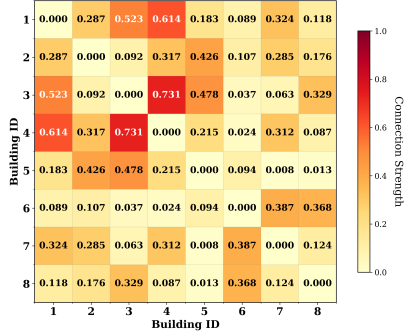


Fig. 6: Building connection weight heatmap showing learned spatial relationships among 8 buildings derived from geographic proximity and attribute similarity for coordinated energy management.

To intuitively understand the spatial and temporal relationships learned by STEMS, in this subsection, we inspect the learned building attention weight matrix and temporal attention. We randomly select a set of buildings which includes 5 residential, 2 commercial and 1 mixed buildings. The building connection weight heatmap (Figure 6) reveals the learned spatial relationships among the 8 buildings in the multi-building energy management system. The visualization demonstrates a heterogeneous connection pattern with connection weights ranging from 0.008 to 0.731, reflecting STEMS's ability to identify coordination opportunities and selective communication strategies. The strongest connections emerge between Buildings 3-4 (0.731) and Buildings 1-4 (0.614),

indicating critical coordination pairs within the residential cluster that enable effective load balancing and energy sharing.

Residential buildings (Buildings 1-5) show varied intra-type connections with moderate-to-strong relationships, demonstrating selective coordination rather than uniform clustering. Commercial buildings (Buildings 6-7) exhibit moderate interconnection (0.387), while the mixed-use building (Building 8) serves as a strategic coordination hub with balanced connections to both building types. Cross-type connections reveal strategic coordination patterns, with notable residential-commercial links such as Buildings 1-7 (0.324) and 4-7 (0.312) enabling load balancing during complementary demand periods. The learned connection weights automatically adapt to changing conditions, strengthening connections between buildings that benefit most from coordination while reducing unnecessary communication overhead.

Then we inspect the temporal attention learned by temporal Transformer module. Figure 7 provides a detailed comparison of temporal attention patterns between residential and commercial buildings, demonstrating how STEMS adapts its attention mechanisms to different building types' operational characteristics. The residential building temporal attention pat-

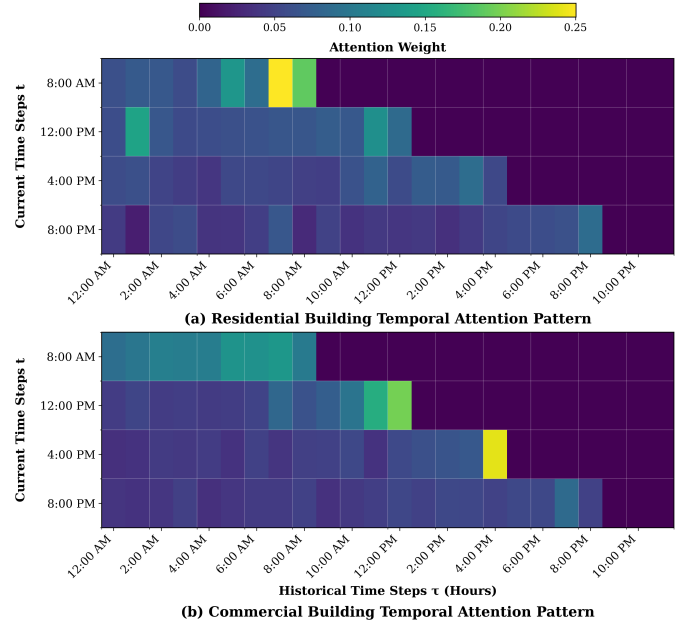


Fig. 7: Building-type-specific temporal attention patterns comparison: (a) Residential building showing distributed attention with evening peaks and lifestyle-driven variability, (b) Commercial building exhibiting concentrated work-hour attention with high regularity and minimal after-hours activity.

tern (Figure 7a) exhibits distinct lifestyle-driven characteristics reflecting typical household energy consumption behaviors. The visualization shows attention weights ranging from 0.05 to 0.15, with distributed attention during morning hours and peak self-attention at 8:00 PM (0.18-0.20), corresponding to residential energy consumption peaks when families engage in evening activities.

In contrast, the commercial building attention pattern (Figure 7b) demonstrates highly structured temporal dependencies

TABLE II: Model Complexity and Scalability Analysis

Building Count	Model Size	Convergence Time
5 buildings	1.51 MB	28 min
8 buildings	1.91 MB	45 min
15 buildings	3.22 MB	158 min

aligned with business operations. The 12:00 PM period exhibits the strongest attention weights (0.15-0.20) during peak business hours, while 8:00 PM shows dramatically reduced attention weights (0.02-0.05), reflecting minimal energy activity after business hours when buildings operate in energy-saving mode.

The complementary nature of these temporal patterns—with residential buildings showing peak activity during evening hours when commercial buildings are inactive—creates optimal opportunities for energy sharing and load balancing through the spatial connections. This spatial-temporal integration demonstrates STEMS’s ability to learn and leverage both the physical similarities between buildings and their temporal operational patterns, enabling load shifting and peak shaving through the spatial network while respecting the natural characteristics of different building types.

#### D. Computational Complexity and Scalability

We then report the computational efficiency and scalability of STEMS across different building network sizes. Table II presents the relationship between building count, model size, and convergence time for scales ranging from 5 to 15 buildings. These scales represent realistic deployment scenarios commonly found in smart building systems, from small residential complexes to medium-sized neighborhoods. The model size scales approximately linearly with building count, primarily due to the independent actor-critic networks required for each building agent. The shared spatial-temporal graph components maintain relatively constant size, contributing to computational efficiency. The model size increases from 1.51 MB for 5 buildings to 1.91 MB for 8 buildings, demonstrating efficient scaling with manageable memory requirements. Convergence time exhibits quadratic growth  $O(N^2)$ , reflecting the computational complexity of spatial-temporal graph learning where message passing scales with the square of building count. Despite this quadratic scaling, absolute convergence times remain practical for real-world deployment. The convergence time increases from 28 minutes for 5 buildings to 158 minutes for 15 buildings, which is acceptable for offline training.

#### E. Ablation Study

Table III analyzes the contribution of each component in the STEMS framework.

The most critical finding is CBF’s role as the primary safety differentiator. Removing CBF increases safety violations from 5.6% to 20.8%—crossing the threshold from acceptable operational risk to unacceptable system reliability. In real building management, this 271% increase represents the difference between regulatory compliance and potential

equipment damage or occupant safety concerns. Notably, CBF achieves this safety improvement with minimal performance cost, maintaining nearly identical economic metrics while dramatically reducing operational risk. The GCN-Transformer architecture serves as the performance foundation, with its removal causing the largest individual degradation (5.1% cost increase, 115% comfort degradation). This reflects the practical reality that without proper spatial-temporal feature representation, coordination mechanisms cannot function effectively. The architecture’s impact on safety violations (121% increase to 12.4%) demonstrates that effective feature learning is prerequisite for both performance optimization and constraint satisfaction in complex multi-building systems. The spatial graph and temporal attention components demonstrate diminishing returns typical of real-world coordination systems. Spatial coordination provides moderate benefits (2.5% cost reduction, 77% comfort improvement from 0.23 to 0.13 discomfort proportion), reflecting the practical challenges of inter-building energy sharing due to transmission losses and grid constraints. Temporal attention shows smaller individual impact (1.3% cost reduction) but proves essential for predictive control, enabling proactive rather than reactive energy management—a crucial capability during peak demand periods.

## IV. RELATED WORK

### A. Building Energy Management Systems

Building energy management systems play a critical role in achieving global carbon neutrality goals, as buildings account for approximately 40% of worldwide energy consumption. Traditional approaches have primarily focused on individual building optimization through three main categories: rule-based control systems that use predefined logic for equipment operation, MPC methods that optimize future actions based on system models [2], [18], and heuristic algorithms that provide practical solutions for complex optimization problems[19].

The integration of renewable energy sources introduces substantial uncertainty due to their intermittent nature, while dynamic electricity pricing and unpredictable occupancy patterns create complex optimization landscapes [1]. These uncertainties make it difficult for traditional model-based approaches to maintain optimal performance. Furthermore, conventional methods typically adopt a single-building optimization perspective, failing to account for the interdependencies and coordination opportunities that exist among multiple buildings in communities or districts. Recent advances in deep learning have led to the emergence of RL based approaches for building energy management [10], [17], [12]. RL methods offer model-free learning capabilities that can adapt to system uncertainties without requiring detailed domain knowledge. Most existing RL applications focus on individual building control due to the inherent complexity and stability concerns of multi-agent systems. This single-building focus leads to suboptimal performance in real-world implementations, where multiple buildings within a community pursue their local objectives independently, often resulting in competitive behaviors that prevent global optimization[9].

TABLE III: Ablation Study Results

Method Variant	Cost	Emission	Avg. Daily Peak	Electricity Consumption	Ramping Rate	Discomfort Proportion	Safety Violations(%)
w/o GCN-Transformer	0.83	0.87	0.86	0.82	0.93	0.28	12.4
w/o Spatial Graph	0.81	0.85	0.84	0.81	0.91	0.23	9.8
w/o Temporal Attention	0.80	0.84	0.83	0.81	0.90	0.19	8.7
w/o CBF Safety	0.78	0.80	0.82	0.79	0.89	0.14	20.8
<b>STEMS</b>	<b>0.79</b>	<b>0.82</b>	<b>0.82</b>	<b>0.80</b>	<b>0.88</b>	<b>0.13</b>	<b>5.6</b>

### B. Multi-Agent Reinforcement Learning

Multi-agent reinforcement learning provides a principled framework for coordinated decision-making in distributed systems where multiple autonomous agents interact within a shared environment [16], [20], [21]. The core challenge lies in handling non-stationarity, where each agent's environment changes as other agents adapt their policies, creating a moving target problem. Classical multi-agent RL algorithms address this through centralized training with decentralized execution methods like MADDPG [16], value function factorization techniques such as QMIX [20], and policy gradient methods that account for multi-agent interactions. Building energy management represents a natural application domain for multi-agent RL due to the distributed nature of building systems and their inherent interdependencies. Distributed residential energy management systems employ multi-agent RL to coordinate household energy scheduling, where each building optimizes its energy consumption while contributing to grid stability [3], [22]. Multi-zone HVAC control leverages multi-agent RL for temperature regulation across building zones, handling occupancy patterns while maintaining thermal comfort [13]. Grid-interactive building coordination uses iterative sequential action selection for effective load shaping and demand response [12]. Federated learning approaches have also emerged to enable collaborative optimization while preserving privacy [23]. However, current multi-agent RL methods lack the ability to effectively model spatial-temporal dependencies among buildings, which limits coordination effectiveness. Spatial dependencies arise from physical coupling between buildings, including thermal transfer, shading effects, and shared infrastructure. Temporal dependencies encompass both short-term dynamics, such as equipment response times and occupancy patterns, and long-term trends including seasonal variations. Graph neural networks have shown promise in capturing spatial relationships in power grids and building clusters [5], [4]. Effective modeling of these spatial-temporal relationships through graph-based representations could enable more informed coordination decisions and enhanced information propagation among agents.

### C. Safe Reinforcement Learning

Safety is a critical concern when deploying RL algorithms in real-world systems, particularly in safety-critical domains such as building energy management [8], [24]. Current safe RL approaches can be categorized into several main directions: constrained optimization methods that integrate safety requirements directly into the learning objective, CBFs that provide mathematical guarantees for constraint satisfaction in contin-

uous control systems, and safe exploration strategies that prevent dangerous actions during the learning process [25]. Recent work has demonstrated the application of safe RL to smart home energy management, where safety constraints include battery state-of-charge limits, temperature comfort bounds, and power consumption limits [7], [6], [11]. However, most existing safe RL methods focus on single-agent scenarios and lack comprehensive frameworks for multi-agent coordination with safety guarantees. The integration of safety constraints with multi-agent coordination presents unique challenges in building energy systems. Distributed safety constraints must be satisfied not only at the individual building level but also at the community and grid levels. Recent surveys highlight that safe RL for power systems remains an active research area with significant gaps in multi-agent scenarios [26]. The combination of spatial-temporal awareness with rigorous safety guarantees in multi-agent building energy management represents a key research direction that requires novel approaches to ensure both coordination effectiveness and safety compliance.

## V. CONCLUSION

In this work, we study the coordinated building energy management problem in multi-building systems with complex spatial-temporal dependencies and safety requirements. We propose STEMS, a safety-constrained multi-agent reinforcement learning framework for coordinated building energy management based on information sharing and cooperative optimization. The GCN-Transformer fusion architecture is introduced to multi-agent RL to enhance agents' spatial-temporal awareness of inter-building relationships and temporal energy patterns. The CBF-based safety shield provides mathematical guarantees for safe operation while maintaining system performance. In experiments, we verify the effectiveness and advantages of our method and each of its components in both safety and efficiency by comparing results with baseline methods across different scenarios, including long-term performance evaluation and extreme weather conditions with diverse building types. The results demonstrate significant improvements in cost, emission and safety violation reduction while maintaining optimal comfort levels. Future work could extend to enhance the robustness of the multi-agent RL algorithm and CBF safety mechanisms with different types of uncertain renewable energy generation, evaluate scalability on larger-scale building networks, and explore the interpretability of learned policies to provide practical insights for building management applications.

## REFERENCES

[1] L. Chen, Y. Hu, R. Wang, X. Li, Z. Chen, J. Hua, A. I. Osman, M. Farghali, L. Huang, J. Li, *et al.*, "Green building practices to integrate

renewable energy in the construction sector: a review," *Environmental Chemistry Letters*, vol. 22, no. 2, pp. 751–784, 2024.

[2] H. Zhang, S. Seal, D. Wu, F. Bouffard, and B. Boulet, "Building energy management with reinforcement learning and model predictive control: A survey," *IEEE Access*, vol. 10, pp. 27 853–27 862, 2022.

[3] A. Kumari, R. Kakkar, S. Tanwar, D. Garg, Z. Polkowski, F. Alqahhani, and A. Tolba, "Multi-agent-based decentralized residential energy management using deep reinforcement learning," *Journal of Building Engineering*, vol. 87, p. 109031, 2024.

[4] N. Haidar, N. Tamani, Y. Ghamri-Doudane, and A. Boujou, "Selective reinforcement graph mining approach for smart building energy and occupant comfort optimization," *Building and Environment*, vol. 228, p. 109806, 2023.

[5] X. Chen, T. Yu, Z. Pan, Z. Wang, and S. Yang, "Graph representation learning-based residential electricity behavior identification and energy management," *Protection and Control of Modern Power Systems*, vol. 8, no. 1, p. 28, 2023.

[6] X. Wang, P. Wang, R. Huang, X. Zhu, J. Arroyo, and N. Li, "Safe deep reinforcement learning for building energy management," *Applied Energy*, vol. 377, p. 124328, 2025.

[7] H. Ding, Y. Xu, B. C. S. Hao, Q. Li, and A. Lentzakis, "A safe reinforcement learning approach for multi-energy management of smart home," *Electric Power Systems Research*, vol. 210, p. 108120, 2022.

[8] L. Brunke, M. Greeff, A. W. Hall, Z. Yuan, S. Zhou, J. Panerati, and A. P. Schoellig, "Safe learning in robotics: From learning-based control to safe reinforcement learning," *Annual Review of Control, Robotics, and Autonomous Systems*, vol. 5, no. 1, pp. 411–444, 2022.

[9] Q. Meng, S. Hussain, F. Luo, Z. Wang, and X. Jin, "An online reinforcement learning-based energy management strategy for microgrids with centralized control," *IEEE Transactions on Industry Applications*, 2024.

[10] C. Guo, X. Wang, Y. Zheng, and F. Zhang, "Real-time optimal energy management of microgrid with uncertainties based on deep reinforcement learning," *Energy*, vol. 238, p. 121873, 2022.

[11] D. Jang, L. Yan, L. Spangher, and C. J. Spanos, "Active reinforcement learning for robust building control," *Proceedings of the AAAI Conference on Artificial Intelligence*, vol. 38, no. 20, pp. 22 150–22 158, Mar. 2024. [Online]. Available: <https://ojs.aaai.org/index.php/AAAI/article/view/30219>

[12] J. R. Vazquez-Canteli, G. Henze, and Z. Nagy, "Marlisa: Multi-agent reinforcement learning with iterative sequential action selection for load shaping of grid-interactive connected buildings," in *Proceedings of the 7th ACM International Conference on Systems for Energy-Efficient Buildings, Cities, and Transportation*, ser. BuildSys '20. New York, NY, USA: Association for Computing Machinery, 2020, p. 170–179. [Online]. Available: <https://doi.org/10.1145/3408308.3427604>

[13] L. Yu, Y. Sun, Z. Xu, C. Shen, D. Yue, T. Jiang, and X. Guan, "Multi-agent deep reinforcement learning for hvac control in commercial buildings," *IEEE Transactions on Smart Grid*, vol. 12, no. 1, pp. 407–419, 2021.

[14] K. Nweye, K. Kaspar, G. Buscemi, T. Fonseca, G. Pinto, D. Ghose, S. Duddukuru, P. Pratapa, H. Li, J. Mohammadi, L. Lino Ferreira, T. Hong, M. Ouf, A. Capozzoli, and Z. Nagy, "Citylearn v2: energy-flexible, resilient, occupant-centric, and carbon-aware management of grid-interactive communities," *Journal of Building Performance Simulation*, vol. 0, no. 0, pp. 1–22, 2024. [Online]. Available: <https://doi.org/10.1080/19401493.2024.2418813>

[15] T. Haarnoja, A. Zhou, P. Abbeel, and S. Levine, "Soft actor-critic: Off-policy maximum entropy deep reinforcement learning with a stochastic actor," in *International conference on machine learning*. Pmlr, 2018, pp. 1861–1870.

[16] R. Lowe, Y. I. Wu, A. Tamar, J. Harb, O. Pieter Abbeel, and I. Mordatch, "Multi-agent actor-critic for mixed cooperative-competitive environments," *Advances in neural information processing systems*, vol. 30, 2017.

[17] H. Zhang, D. Wu, and B. Boulet, "Metaems: A meta reinforcement learning-based control framework for building energy management system," 2022. [Online]. Available: <https://arxiv.org/abs/2210.12590>

[18] J. Berberich and F. Allgöwer, "An overview of systems-theoretic guarantees in data-driven model predictive control," *Annual Review of Control, Robotics, and Autonomous Systems*, vol. 8, 2024.

[19] M. Ghalambaz, R. J. Yengejeh, and A. H. Davami, "Building energy optimization using grey wolf optimizer (gwo)," *Case Studies in Thermal Engineering*, vol. 27, p. 101250, 2021.

[20] T. Rashid, M. Samvelyan, C. S. de Witt, G. Farquhar, J. Foerster, and S. Whiteson, "Qmix: Monotonic value function factorisation for deep multi-agent reinforcement learning," in *ICML 2018*, 2018, pp. 4292–4301. [Online]. Available: <https://proceedings.mlr.press/v80/rashid18a.html>

[21] C. Yu, A. Velu, E. Vinitsky, J. Gao, Y. Wang, A. Bayen, and Y. Wu, "The surprising effectiveness of ppo in cooperative multi-agent games," *Advances in neural information processing systems*, vol. 35, pp. 24 611–24 624, 2022.

[22] L. Ding, Y. Cui, G. Yan, Y. Huang, and Z. Fan, "Distributed energy management of multi-area integrated energy system based on multi-agent deep reinforcement learning," *International Journal of Electrical Power & Energy Systems*, vol. 157, p. 109867, 2024.

[23] Y. Xia, X. Wang, X. Yin, W. Bo, L. Wang, S. Li, and K. Li, "Federated accelerated deep reinforcement learning for multi-zone hvac control in commercial buildings," *IEEE Transactions on Smart Grid*, 2025.

[24] S. Gu, L. Yang, Y. Du, G. Chen, F. Walter, J. Wang, and A. Knoll, "A review of safe reinforcement learning: Methods, theories and applications," *IEEE Transactions on Pattern Analysis and Machine Intelligence*, 2024.

[25] G. Thomas, Y. Luo, and T. Ma, "Safe reinforcement learning by imagining the near future," *Advances in Neural Information Processing Systems*, vol. 34, pp. 13 859–13 869, 2021.

[26] T. Su, T. Wu, J. Zhao, A. Scaglione, and L. Xie, "A review of safe reinforcement learning methods for modern power systems," *Proceedings of the IEEE*, 2025.